Linear optics based nanoscopy

Aviram Gur,[1] Dror Fixler,[1] Vicente Micó,[2] Javier Garcia,[2] and Zeev Zalevsky[1,*]

[1]*School of Engineering, Bar-Ilan University, 52900, Ramat-Gan, Israel*
[2]*Departamento de Óptica, Univ. Valencia, C/Dr. Moliner, 50, 46100 Burjassot, Spain*
**zalevsz@macs.biu.ac.il*

Abstract: Classically, optical systems are considered to have a fundamental resolution limit due to wave nature of light. This article presents a novel method for observing sub-wavelength features in a conventional optical microscope using linear optics. The operation principle is based on a random and time varying flow of nanoparticles moving in proximity to the inspected sample. Those particles excite the evanescent waves and couple them into harmonic waves. The sub-wavelength features are encoded and later on digitally decoded by proper image processing of a sequence of images. The achievable final resolution limit corresponds to the size of the nanoparticles. Experimental proof of principle validation of the technique is reported.

OCIS codes: (100.6640) Superresolution; (100.2000) Digital image processing; (200.4740) Optical processing.

References and Links

1. E. Abbe, "Beiträge zur Theorie des Mikroskops und der mikroskopischen Wahrnehmung," Archiv für Mikroskopische Anatomie **9**(1), 413–418 (1873).
2. Y. Garini, B. J. Vermolen, and I. T. Young, "From micro to nano: recent advances in high-resolution microscopy," Curr. Opin. Biotechnol. **16**(1), 3–12 (2005).
3. I. J. Cox, and C. J. R. Sheppard, "Information capacity and resolution in an optical system," J. Opt. Soc. Am. A **3**(8), 1152–1158 (1986).
4. W. Lukosz, "Optical systems with resolving powers exceeding the classical limit," J. Opt. Soc. Am. **56**(11), 1463–1472 (1966).
5. Z. Zalevsky, D. Mendlovic, and A. W. Lohmann, Optical systems with improved resolving power, Ch. 4, Progress in Optics, vol XL, ed E. Wolf, Elsevier (2000).
6. Z. Zalevsky, and D. Mendlovic, Optical Super Resolution, Springer, New York (2002).
7. S. A. Alexandrov, T. R. Hillman, T. Gutzler, and D. D. Sampson, "Synthetic aperture fourier holographic optical microscopy," Phys. Rev. Lett. **97**(16), 168102 (2006).
8. Y. Kuznetsova, A. Neumann, and S. R. J. Brueck, "Imaging interferometric microscopy-approaching the linear systems limits of optical resolution," Opt. Express **15**(11), 6651–6663 (2007).
9. V. Micó, Z. Zalevsky, C. Ferreira, and J. García, "Superresolution digital holographic microscopy for three-dimensional samples," Opt. Express **16**(23), 19260–19270 (2008).
10. E. Betzig, J. K. Trautman, T. D. Harris, J. S. Weiner, and R. L. Kostelak, "Breaking the diffraction barrier: optical microscopy on a nanometric scale," Science **251**(5000), 1468–1470 (1991).
11. S. W. Hell, and J. Wichmann, "Breaking the diffraction resolution limit by stimulated emission: stimulated-emission-depletion fluorescence microscopy," Opt. Lett. **19**(11), 780–782 (1994).
12. V. Westphal, and S. W. Hell, "Nanoscale resolution in the focal plane of an optical microscope," Phys. Rev. Lett. **94**(14), 143903 (2005).
13. M. G. L. Gustafsson, "Nonlinear structured-illumination microscopy: wide-field fluorescence imaging with theoretically unlimited resolution," Proc. Natl. Acad. Sci. U.S.A. **102**(37), 13081–13086 (2005).
14. S. Bretschneider, C. Eggeling, and S. W. Hell, "Breaking the diffraction barrier in fluorescence microscopy by optical shelving," Phys. Rev. Lett. **98**(21), 218103 (2007).
15. T. D. Lacoste, X. Michalet, F. Pinaud, D. S. Chemla, A. P. Alivisatos, and S. Weiss, "Ultrahigh-resolution multicolor colocalization of single fluorescent probes," Proc. Natl. Acad. Sci. U.S.A. **97**(17), 9461–9466 (2000).
16. M. J. Rust, M. Bates, and X. Zhuang, "Sub-diffraction-limit imaging by stochastic optical reconstruction microscopy (STORM)," Nat. Methods **3**(10), 793–796 (2006).
17. E. Betzig, G. H. Patterson, R. Sougrat, O. W. Lindwasser, S. Olenych, J. S. Bonifacino, M. W. Davidson, J. Lippincott-Schwartz, and H. F. Hess, "Imaging intracellular fluorescent proteins at nanometer resolution," Science **313**(5793), 1642–1645 (2006).

#128986 - $15.00 USD Received 25 May 2010; revised 20 Aug 2010; accepted 23 Aug 2010; published 5 Oct 2010

18. S. T. Hess, T. P. K. Girirajan, and M. D. Mason, "Ultra-high resolution imaging by fluorescence photoactivation localization microscopy," Biophys. J. **91**(11), 4258–4272 (2006).
19. D. Semwogerere, and E. R. Weeks, Confocal Microscopy, Encyclopedia of Biomaterials and Biomedical Engineering, Taylor & Francis (2005).
20. W. R. Zipfel, R. M. Williams, and W. W. Webb, "Nonlinear magic: multiphoton microscopy in the biosciences," Nat. Biotechnol. **21**(11), 1369–1377 (2003).
21. S. Hell, and E. H. K. Stelzer, "Fundamental improvement of resolution with a 4Pi-confocal fluorescence microscope using two-photon excitation," Opt. Commun. **93**(5-6), 277–282 (1992).
22. M. G. L. Gustafsson, D. A. Agard, and J. W. Sedat, "I5M: 3D widefield light microscopy with better than 100 nm axial resolution," J. Microsc. **195**(1), 10–16 (1999).
23. M. G. L. Gustafsson, "Surpassing the lateral resolution limit by a factor of two using structured illumination microscopy," J. Microsc. **198**(2), 82–87 (2000).
24. J. T. Frohn, H. F. Knapp, and A. Stemmer, "True optical resolution beyond the Rayleigh limit achieved by standing wave illumination," Proc. Natl. Acad. Sci. U.S.A. **97**(13), 7232–7236 (2000).
25. D. Toomre, and D. J. Manstein, "Lighting up the cell surface with evanescent wave microscopy," Trends Cell Biol. **11**(7), 298–303 (2001).
26. L. Shao, B. Isaac, S. Uzawa, D. A. Agard, J. W. Sedat, and M. G. L. Gustafsson, "I5S: wide-field light microscopy with 100-nm-scale resolution in three dimensions," Biophys. J. **94**(12), 4971–4983 (2008).
27. O. Gliko, G. D. Reddy, B. Anvari, W. E. Brownell, and P. Saggau, "Standing wave total internal reflection fluorescence microscopy to measure the size of nanostructures in living cells," J. Biomed. Opt. **11**(6), 064013 (2006).
28. K. Fujita, M. Kobayashi, S. Kawano, M. Yamanaka, and S. Kawata, "High-resolution confocal microscopy by saturated excitation of fluorescence," Phys. Rev. Lett. **99**(22), 228105 (2007).
29. R. Fiolka, M. Beck, and A. Stemmer, "Structured illumination in total internal reflection fluorescence microscopy using a spatial light modulator," Opt. Lett. **33**(14), 1629–1631 (2008).
30. E. Baleine, and A. Dogariu, "Variable coherence scattering microscopy," Phys. Rev. Lett. **95**(19), 193904 (2005).
31. T. Kalkbrenner, U. Håkanson, A. Schädle, S. Burger, C. Henkel, and V. Sandoghdar, "Optical microscopy via spectral modifications of a nanoantenna," Phys. Rev. Lett. **95**(20), 200801 (2005).
32. G. Maire, F. Drsek, J. Girard, H. Giovannini, A. Talneau, D. Konan, K. Belkebir, P. C. Chaumet, and A. Sentenac, "Experimental demonstration of quantitative imaging beyond Abbe's limit with optical diffraction tomography," Phys. Rev. Lett. **102**(21), 213905 (2009).
33. Z. Zalevsky, E. Saat, S. Orbach, V. Mico, and J. Garcia, "Exceeding the resolving imaging power using environmental conditions," Appl. Opt. **47**(4), A1–A6 (2008).
34. Z. Zalevsky, E. Fish, N. Shachar, Y. Vexberg, V. Mico, and J. Garcia, "Super-resolved imaging with randomly distributed, time- and size-varied particles," J. Opt. A, Pure Appl. Opt. **11**(8), 085406 (2009).

1. Introduction

In 1873, Ernst Abbe discovered that a lens-based optical system cannot distinguish between details having lateral separation smaller than half the optical wavelength (λ) divided by the numerical aperture (NA) [1]. Hence, the observation of details beyond the bounds imposed by Abbe's diffraction theory has been of unquestionable interest in the life sciences and engineering [2]. One can distinguish between two different directions when surpassing the diffraction limit, or in other words, to achieve super resolution. The first one is related with improving the resolution limit provided by the Abbe's theory up to the maximum value imposed by the diffraction of light. On the other hand, the second direction is aimed to achieve spatial resolution far beyond the barrier imposed by the diffraction of light. In the former case, propagating (harmonic) waves can be collected up to a maximum spatial frequency value of NA/λ or $2NA/\lambda$ (depending on the use of coherent or incoherent illumination, respectively), while the latter case implies the obtaining of sub-wavelength features incoming from evanescent (non propagating) waves.

Regarding the first type of methods, super resolved techniques capable of beating the Abbe's diffraction limit while scoping with harmonic waves are based on the invariance theorem provided by information theory about the number of degrees of freedom (domains) in imaging systems [3]. Essentially, the encoding of the spatial-frequency object information (spatial degree of freedom) into another domain allows its transmission through the optical system and, thus, the reconstruction of a super resolved image by proper decoding process. Some examples for that can be found in the bibliography [4–6]. In that sense, time

#128986 - $15.00 USD Received 25 May 2010; revised 20 Aug 2010; accepted 23 Aug 2010; published 5 Oct 2010

multiplexing is one of the most applicable approaches for achieve super resolution imaging in microscopy [7–9].

On the other hand, different methods had been proposed mainly throughout the past two decades to beating the diffraction barrier while allowing nanometric scale imaging. Near-field scanning optical microscopy [10] uses an ultra sharp tip in the vicinity of the object to scan and collect point by point the sub-wavelength information. Instead of a physical tip, stimulated emission depletion (STED) microscopy [11,12] and non-linear (saturated) structured illumination microscopy (SSIM) [13] utilize a tiny light spot or line as excitation pattern to scan the samples, respectively. Sub-wavelength information can be attainable because the excitation pattern becomes sharper than in conventional fluorescence microscopy due to stimulated emission and nonlinearity effect in the fluorophore. Another similar method is based on reversible saturable optically linear fluorescence transition (RESOLFT) microscopy in which the fluorescent molecules can be reversibly photo-switched between a fluorescent and a dark state [14]. Other examples of approaches capable of beating the diffraction barrier in fluorescence microscopy are based on single fluorescent molecule localization allowing nanometer resolution of individual molecules [15–18]. Using this kind of strategies, the lateral resolution limit can be reduced down to 20-50 nm.

However, all of those methods [11–18] are based on labelling the sample with some special (photoswitchable or photoaactivated or reversible) fluorophore. Thus, they are dependent on the photophysics or photochemistry of the fluorophore. On the contrary, there are other methods that can be applied under general imaging purposes such as confocal [19] and multiphoton [20] microscopy, 4Pi [21] and I5M (image interference microscopy combined with incoherent interference illumination microscopy) [22], structured illumination microscopy [23], standing wave illumination [24], total internal reflection fluorescence microscopy [25], and combinations between them [26–29]. Such methods have enabled lateral resolutions in the 100 nm scale.

In the last years, new microscopic approaches have emerged to provide sub-wavelength resolutions [30–32]. Here, we present a novel approach capable of sub-wavelength nanoscopic imaging working outside the fluorescent field and using a standard far-field microscope. It is based on a time multiplexing encoding-decoding process realized through a random sparse dynamic flow of nanoparticles. The nanoparticles provide the encoding of sub-wavelength features by coupling the evanescent waves into harmonic ones in such a way that can be detected in the far field regime. Although the proposed numerical manipulation was previously reported in the frame of super resolution by beating the Abbe's diffraction limit for general imaging systems [33,34], now it is demonstrated for the first time as microscopy super resolution method surpassing the diffraction barrier of light where the final resolution improvement approaches the diameter of the nanoparticles used in the experiment. Thus, super resolved nanoscale optical imaging is achieved without the need of labeling with fluorophores the inspected sample and without any non-linear effect. The proposed approach fills the gap existing in the applicability of optical methods for the analysis and quality control of semiconductor industry samples such as lithographic masks, integrated circuits, thin film nanopatterning etc.

2. Theoretical description

Qualitatively, the proposed methodology starts when capturing a set of diffraction limited images from the input object having a given random nanoparticles distribution that changes from one image to the immediately following one. To allow this, we use an upright microscope and a water immersion microscope objective with the nanoparticles in water suspension. Thus, the random nanoparticles distribution is modified due to the Brownian motion of the particles in the fluid and plays the role of encoding mask. Then, the decoding mask is numerically estimated having no a priori assumption on the generated random flow of nanoparticles and according to the following procedure: the diffraction limited image of the

#128986 - $15.00 USD Received 25 May 2010; revised 20 Aug 2010; accepted 23 Aug 2010; published 5 Oct 2010

object is subtracted from each single image and the centers of the blurred spots are allocated. This operation is possible since the random distribution of the nanoparticles is sparse. Note that, since the nanoparticles are beyond the diffraction limit of the microscope lens, they will appear as blurred spots in the recorded images. Moreover, only such nanoparticles in close contact with the input sample are taken into account in the digital process because those ones at different axial distances will appear misfocused (outside the depth of field of the microscope lens) and not blurred. As a result, a decoding mask is synthesized for each recorded image corresponding with a given nanoparticles distribution where the gray level representative of each nanoparticle is proportional to the input sample transmittance at that point. After that, we multiply each image by its corresponding decoding mask and sum all the images. Finally, we subtract the diffraction limited image of the object from that summation and obtain the super resolved reconstruction having sub-wavelength details.

Assuming for simplicity a one-dimensional (1-D) mathematical treatment in our theoretical analysis (the expansion for the two-dimensional (2-D) case is straightforward) and denoting by s(x) the original high resolution distribution of the input sample containing sub-wavelength features which we wish to resolve, by p(x) the PSF of our microscope system, and by f(x,t) the randomly dynamic sparse distribution of flowing nanoparticles (x and t are the spatial and the temporal coordinates, respectively), each diffraction limited image in the sequence that is captured by the camera equals to the formulation of Eq. (1):

$$\int_{x'} s(x') f(x',t) p(x-x') dx' \tag{1}$$

where the nanoparticles distribution f(x,t) varies in time according to its Brownian motion. Then, the decoding pattern is numerically extracted according with the previously explained procedure and the reconstruction r(x) is obtained by applying the following calculation

$$r(x) = \int_t \left[\int_{x'} s(x') f(x',t) p(x-x') dx' \right] \tilde{f}(x,t) dt \tag{2}$$

where $\tilde{f}(x,t)$ is the digitally estimated decoding pattern. Since the nanoparticles distribution is random, we can assume that the encoding/decoding pattern verifies

$$\int_t f(x',t) \tilde{f}(x,t) dt = \frac{1}{\sqrt{2\pi}\sigma} \exp\left(\frac{-(x'-x)^2}{2\sigma^2} \right) + \kappa \tag{3}$$

being κ a constant and σ a coefficient that when it goes to zero the first term in the right wing of Eq. (1) becomes the delta function of Dirac (denoted as δ):

$$\lim_{\sigma \to 0} \frac{1}{\sqrt{2\pi}\sigma} \exp\left(\frac{-(x'-x)^2}{2\sigma^2} \right) = \delta(x'-x) \tag{4}$$

By changing the integration order in Eq. (2) and using Eq. (3) we finally can write:

$$\begin{aligned} r(x) &= \int_{x'} s(x') \left[\int_t \tilde{f}(x',t) f(x,t) dt \right] p(x-x') dx' = \int_{x'} s(x') \frac{1}{\sqrt{2\pi}\sigma} \exp\left(\frac{-(x'-x)^2}{2\sigma^2} \right) p(x-x') dx' \\ &+ \kappa \int_{x'} s(x') p(x-x') dx' = s(x) * \left[\frac{1}{\sqrt{2\pi}\sigma} \exp\left(\frac{-x^2}{2\sigma^2} \right) \cdot p(x) \right] + \kappa \int_{x'} s(x') p(x-x') dx' \end{aligned} \tag{5}$$

where * denotes convolution operation. Making an analysis of Eq. (5) shows that the resulted reconstruction r(x) equals to the high resolution input sample distribution s(x) blurred by a function having spatial width of σ (thus σ is the coefficient determines the final reconstructed

#128986 - $15.00 USD Received 25 May 2010; revised 20 Aug 2010; accepted 23 Aug 2010; published 5 Oct 2010

resolution) and summed with its diffraction limited (low band pass filtering) version. In the ideal case when σ goes to zero one obtains

$$r(x)=\int_{x'} s(x')\left[\int_t \tilde{f}(x',t)\,f(x,t)\,dt\right]p(x-x')\,dx'=\int_{x'} s(x')\,\delta(x'-x)\,p(x-x')\,dx' \\ +\kappa\int_{x'} s(x')\,p(x-x')dx'=s(x)\,p(0)+\kappa\int_{x'} s(x')\,p(x-x')dx' \tag{6}$$

here the first term of the reconstruction r(x) equals to the high resolution input sample distribution s(x) multiplied by a constant p(0) and thus indeed in this case the reconstruction of the high spatial frequencies is ideal.

Note that several factors determine the final resolution of the reconstruction. However, the size of the nanoparticles is one of the main factors to determine the final resolution limit. The size of those particles correspond to the spatial width denoted by σ.

What Eq. (5) suggests is that theoretically unlimited reconstructed resolution is achievable by subtracting the diffraction limited version from the obtained reconstruction. By "unlimited" we mean down to the size of the nanoscale particles used in the encoding process. And since we apply a flow of nanoscale particles, the proposed technique may be used to construct an optical nanoscope.

3. Experimental validation

The proposed optical nanoscope has been tested in our laboratory validating its working principle. In this Section, we show proof of principle validation of the proposed approach. We used a standard Olympus BX51 upright microscope with a 60X water immersion Olympus microscope objective with a NA equal to 1. We have selected a microscope lens having a 1.0NA to directly ascribe all the new resolvable object details when performing the proposed approach with subwavelength object information. Figure 1 shows a picture of the experimental setup. As illumination light we use broad band white light incoming from the halogen lamp of the own microscope illumination system. However in order to adjust the experimental setup, we insert in the microscope embodiment a broad band interference filter (Edmund Optics 950nm with 50nm of FWHM bandwidth). Indeed using shorter wavelength will produce better resolution limit as well as better sensitivity of the imaging camera. However, due to practical limitations of the equipment we had in our lab (the type of interference filters we had) and since for the purpose of proof of principle the exact wavelength is not critical, we used in our experiments the wavelength of 950nm.

#128986 - $15.00 USD Received 25 May 2010; revised 20 Aug 2010; accepted 23 Aug 2010; published 5 Oct 2010

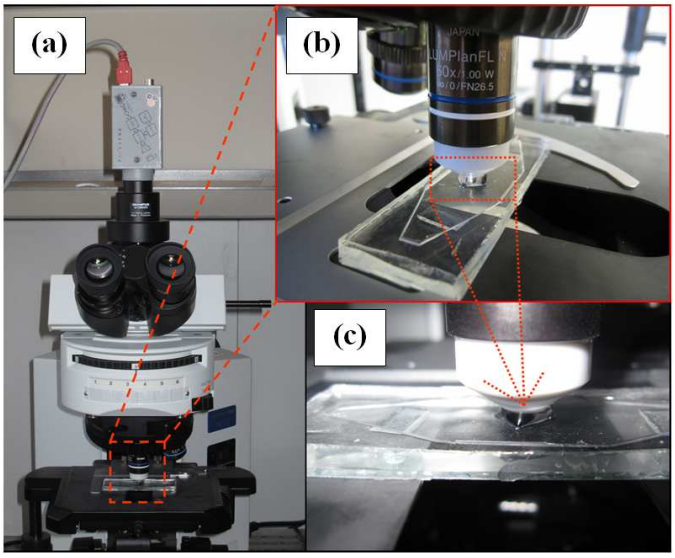

Fig. 1. Experimental layout. (a) Olympus BX51 Microscope station, (b) 60X water immersion lens with NA = 1, and (c) water droplet containing gold nanoparticles flowing in proximity to the inspected sample.

As input sample we use specially manufactured resolution test target: a silicon wafer containing spatial features larger as well as smaller than the optical wavelength that were fabricated using focused ion beam (FIB) system. The opaque details of the test target are divided in 4 groups, each one of them having 3 different elements, and each element composed by 3 different horizontal and vertical bars having the same width. The gap between the bars varied from 100 to 200nm in steps of 20nm at the 6 bars groups appearing in the upper two lines of the target and 250-500nm in steps of 50nm at the 6 bars groups appearing in the third and the fourth line of the target. Nevertheless, the distance between opaque bars does not equals with the bar width. An image of the resolution test target taken with scanning electron microscopy (SEM) is presented in Fig. 2.

In the experiments we used 30μl SPI-Mark unconjugated gold particles with diameter of 200nm. A set of 400 images were captured in the whole sequence. The camera we used was Pixelink PL-A741-E (PixeLINK, Ottawa, ON, 6.7μm square pixels) in a frame rate of 130 frames per second, approximately. In each image the random distribution of the particles varied due to their Brownian flow in the medium. The number and the positions of the particles in each captured frame are estimated numerically from the set of diffraction limited images. The average number of particles for each frame was approximately 240 which means that we had approximately 1.2 particles/μm^2.

The algorithm included digital allocation of the center of each particle in every frame and construction of a decoding pattern with spots corresponding to the locations of those centers. Then each low resolution frame was multiplied by the corresponding decoding pattern. Low resolution diffraction limited image (the second term in the right wing of Eq. (6) was subtracted from each single image. All processed images were summed together to yield the reconstructed high resolution image.

#128986 - $15.00 USD Received 25 May 2010; revised 20 Aug 2010; accepted 23 Aug 2010; published 5 Oct 2010

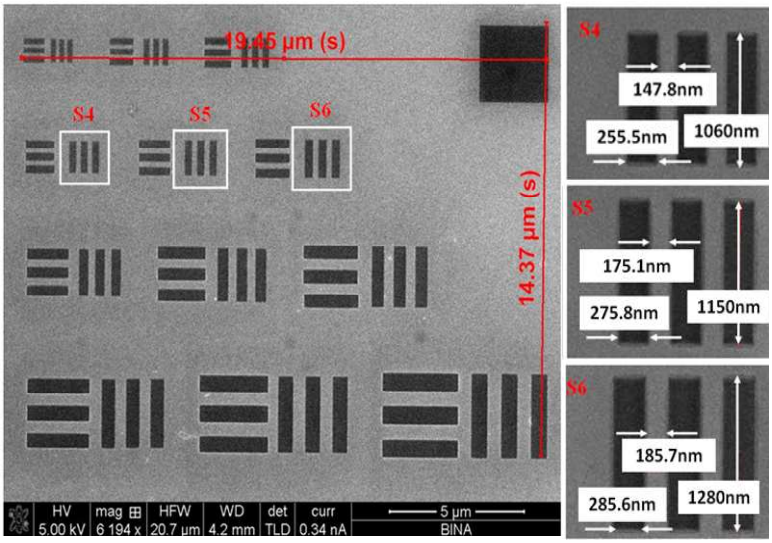

Fig. 2. SEM image of the fabricated resolution test target (up), and magnification of the elements S4-S5-S6 marked with a white square in the upper image (down).

Note that increasing the number of the frames provides better quality of the image not in the sense of resolution improvement but rather in the obtainable coverage of the field of view, i.e. in obtaining the super resolved image in more regions of the field of view. The larger the number of frames the higher is the mean area of coverage. The dependence is as follows: if we denote by $\eta^{(N)}$ the accumulative percentage for the coverage of the field of view by the nanoparticiples after accumulating N frames (and thus the region in the field of view where the super resolved reconstruction is obtained) and by β the percentage of coverage in a single frame then we have:

$$\begin{aligned} \eta^{(N)} &= \eta^{(N-1)}\left(1-\beta\right)+\beta \qquad N \geq 2 \\ \eta^{(1)} &= \beta \end{aligned} \tag{7}$$

The plot of the accumulative portion for the coverage of the field of view versus the number of frames that were in use is seen in Fig. 3 while in this simulation β was chosen to be 0.005 (approximately corresponding to the coverage obtained by 240 nanoparticles per frame).

#128986 - $15.00 USD Received 25 May 2010; revised 20 Aug 2010; accepted 23 Aug 2010; published 5 Oct 2010

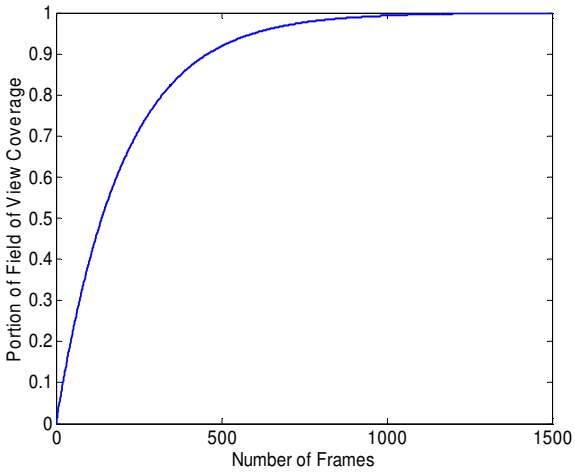

Fig. 3. Plot of the accumulative portion for the coverage of the field of view versus the number of frames that were in use.

Figure 4(a) presents the diffraction limited image of the particles distribution without the resolution target while Fig. 4(b) shows one diffraction limited image of our target out of the sequence captured by the camera (with the flow of the particles). In Fig. 4(c) one may see the video movie presenting the flow of the nanoparticles on top of the inspected resolution target.

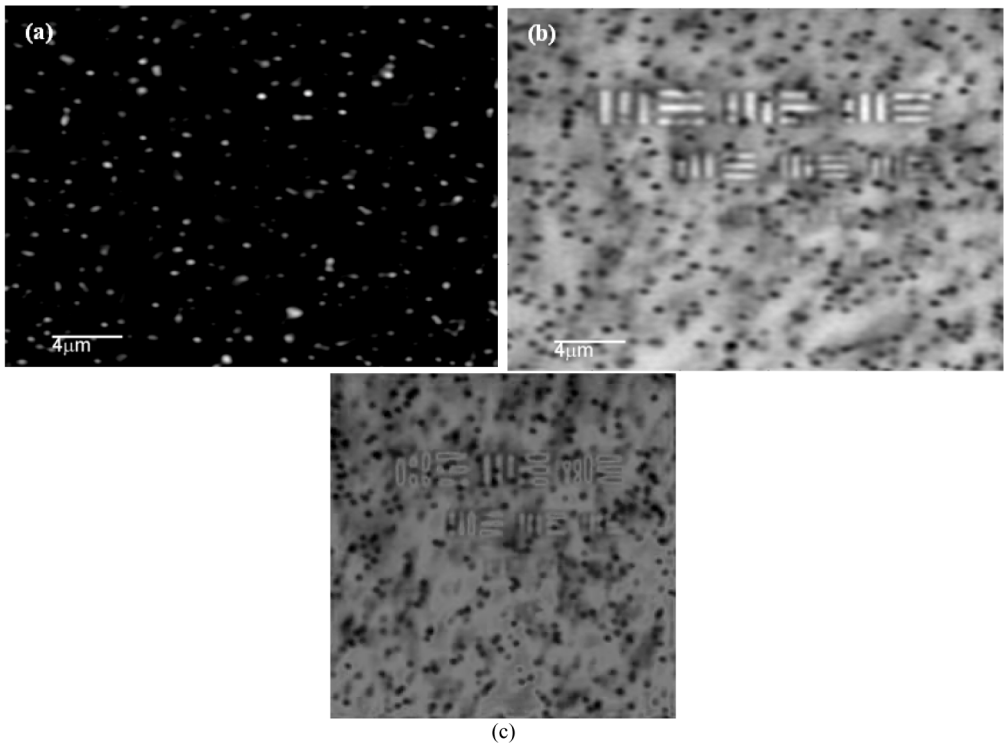

(c)

Fig. 4. (Media 1) (a) Diffraction limited image of the nanoparticles distribution, and (b) one diffraction limited image of the resolution target (with the particles) captured by the camera. (c). The movie presenting the flow of the nanoparticles on top of the inspected resolution target.

#128986 - $15.00 USD Received 25 May 2010; revised 20 Aug 2010; accepted 23 Aug 2010; published 5 Oct 2010

Figure 5(a) presents the diffraction limited image of the target which averaged the entire set of captured images. This image is important as part of the numerical process for extracting the decoding pattern and corresponds with the conventional resolution image provided by the microscope lens. According to the theoretical prediction, the resolution limit R provided by the system is 475 nm incoming from the relation: $R = \lambda/(2NA)$. As one may see, the last resolved element is marked with a white rectangle and corresponds to bars having a pitch of 600nm coming from a width of 350nm and separated by a gap of 250nm. Element S6 is just in the limit of resolution (pitch equal to 471.3nm) but not resolved. Finally, Fig. 5(b) depicts the super resolved reconstruction when performing the proposed approach. One may see that sub-wavelength features corresponding with the elements labeled as S6-S5-S4, which cannot be seen in Fig. 5(a), become now distinguishable in Fig. 5(b). In order to further demonstrate the resolution improvement in the lower part of the Fig. 5(a) as well as 5(b) we zoom on several demonstrative features of the obtained images. The reason why some bars of the super resolved image are not resolved while other are (see for instance the vertical bars on Element S4) is due to the random Brownian motion of the nanoparticles does not sweep enough such area as one can see in the video movie.

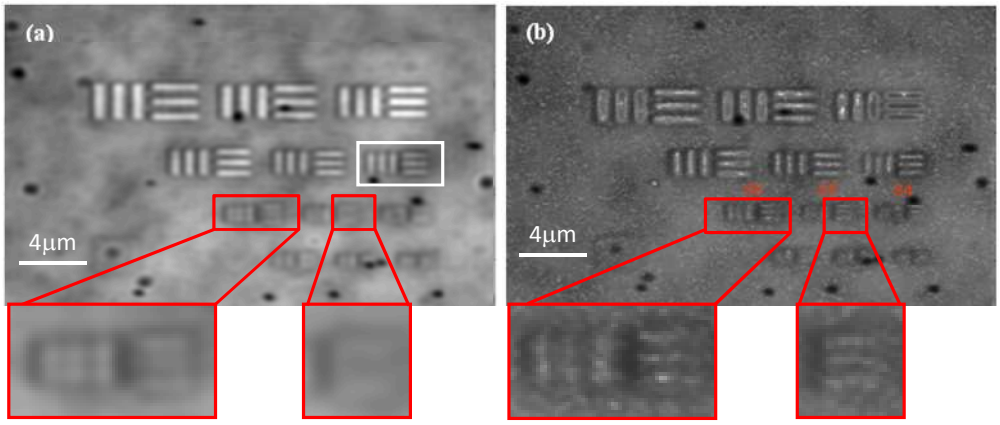

Fig. 5. (a) Diffraction limited image of the resolution test target obtained when averaging the entire set of captured images, and (b) super resolved reconstruction containing sub-wavelength details.

This situation is clearer in Fig. 6 where a comparison of the averaged plot along the horizontal lines of elements S4-S5-S6 in both, the conventional and the super resolved image is presented. Note that some of the nanoparticles were glued to the resolution test target [see Fig. 5(a) and (b)]. This is the reason why those nanoscale particles are not removed in the final reconstruction.

Note that as previously explained using smaller nanoparticles is better in the sense of resolution improvement. However, smaller particles are also lighter and thus they will not flow in sufficient proximity to the object and thus will not produce the required encoding. In addition, since the proposed nanoscope uses conventional diffraction limited lenses, the image of the nanoparticles becomes as much blurred as lower the size is. This problem defines a more sparse distribution of nanoparticles, as the particles decrease in size, in order to allocate their centers. Also, their contrast and visibility is reduced and consequently the task of allocating their centers and constructing the decoding pattern is becoming more complex. This fact also increases the time to achieve a wide field super resolution image.

#128986 - $15.00 USD Received 25 May 2010; revised 20 Aug 2010; accepted 23 Aug 2010; published 5 Oct 2010

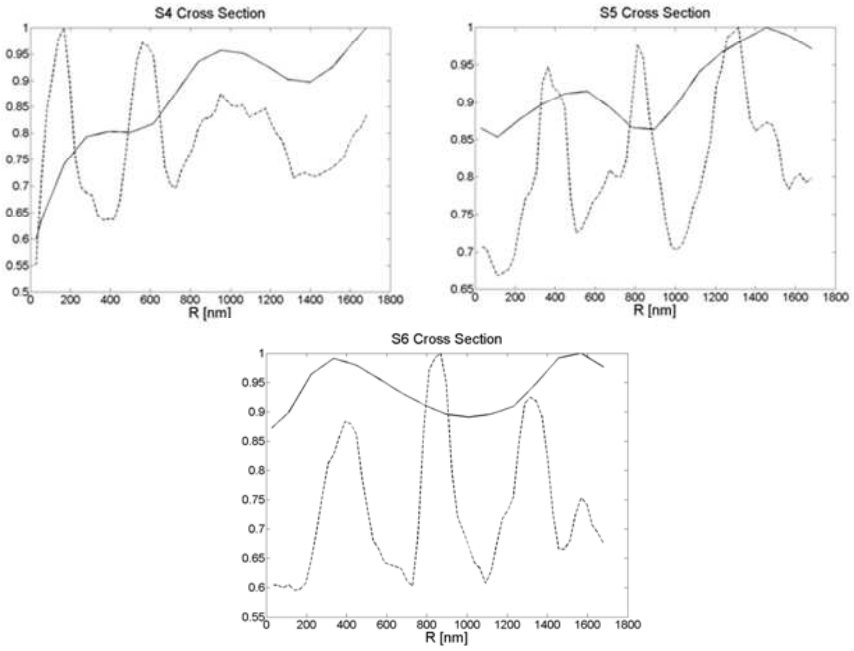

Fig. 6. Comparison of averaged plots of unresolved (solid line) and super resolved (dashed line) elements S4, S5 and S6 in the resolution test target.

4. Conclusions

In summary, proof of principle validation of a linear optical nanoscope capable of provide sub-wavelength super resolution allowing nanoscopic imaging has been presented. The main advantages of the proposed system are related with: first, a conventional transmission optical working principle; second, a variable, adjustable and unlimited resolution gain depending on the critical size of the inspected sample by only selecting the diameter of the nanoparticles; third, no complex hardware are required since the random nanoparticles movement is provided by Brownian flow motion; fourth, no intense illumination of external laser for imaging the sample; and fifth, it is simple and although validation using silicon based resolution target has been presented, more complex studies including biological samples are in process.

The main trade off concerning the proposed method is the selection of the size of the nanoparticles. There is no problem concerning nanoparticles diameters in the range of 50 nm. However, since the proposed nanoscope uses conventional diffraction limited lenses, the image of the nanoparticles becomes as much blurred as the lower the size is. This problem defines a more sparse distribution of nanoparticles as the particles decrease in size in order to allocate the centers. Consequently, this fact increases the time to achieve a wide field super resolution image.

#128986 - $15.00 USD Received 25 May 2010; revised 20 Aug 2010; accepted 23 Aug 2010; published 5 Oct 2010